

# On the Influence of the Underlying Network Topology on Optical Telecommunication Network Availability under Shared Risk Link Group Failures

Vedran Miletić\*, Dimitris Maniadakis†, Branko Mikac‡, Dimitris Varoutas†

\*University of Rijeka Department of Informatics

Rijeka, Croatia

*vmiletic@inf.uniri.hr*

†University of Athens Dept. of Informatics and Telecommunications

Athens, Greece

*{D.Maniadakis, D.Varoutas}@di.uoa.gr*

‡University of Zagreb Faculty of Electrical Engineering and Computing

Zagreb, Croatia

*branko.mikac@fer.hr*

**Abstract**—Network availability is of paramount importance in optical telecommunication networks. Their rising connectivity and consequently their availability is compromised by link and node failures, usually due to physical force (e.g. digging, earthquake or fire). Single link failures can in turn cause multiple failures in case a failure hits a shared risk link group (SRLG), which is a group of logically distinct links sharing a common physical resource, be it a cable or a conduit. The number and length of SRLGs, as well as the characteristics of the underlying physical topology can significantly affect network availability. Especially, the physical topology can be represented by realistic synthetic graphs which are created by numerous geographic graph generators. This work describes the implementation and usage of six different physical topology models (Random Geometric, Gabriel, Relative Neighborhood, K-Nearest Neighbor, Waxman and Spatial Barabási-Albert) for investigation of the influence of the underlying topology on the optical telecommunication network availability. Network availability is estimated using Monte Carlo simulations based on a model of optical telecommunication network implemented by network simulator ns-3. Scenarios utilizing six topology models both in absence and presence of SRLGs are studied, and the optical network availability sensitivity to the underlying physical network topology is presented as the main result.

**Index Terms**—availability, graph theory, Monte Carlo simulation, network topology, ns-3, optical network failures, shared risk link groups

## I. INTRODUCTION

Researchers in the telecommunications field often need to assess new algorithms and protocols over realistic topologies. So far, they have widely used topologies that are either regular, e.g. tree, mesh, for analytic studies of algorithmic performance, or synthetic randomly generated ones in the case of running simulations. Even more, reference topologies [1], [2] or instances of real topologies [3]–[6] are employed wherever available, since telecom operators are usually reluctant to share such information for business competitiveness and security reasons (e.g. to aggravate physical-layer attacks).

However, as real-world topology data are becoming more and more available, the structural and geographic properties of telecommunication networks are analyzed in order to characterize and model such topologies, mainly making use of graph theory tools. Despite the engineers' overriding role in the case of networks, emergent and unplanned topological traits usually appear in both the logical [7] and the physical level [8]. It has been found that the physical topologies can rarely be described by traditional patterns such as star, bus, ring, hierarchical or full mesh graphs and thus a variety of approaches from complex network theory have been discussed lately on the formation of appropriate network models. Recently, Çetinkaya et al. evaluated the fitness of geographical graph generators for modeling physical level topologies [9]. They evaluated four geographical graph models (Gabriel, geometric, population-weighted geographical threshold, Waxman) and drew to the conclusion that while none of these models capture the structure of real networks perfectly, though Gabriel graphs best capture grid-like structure of physical level topologies.

It is natural to expect that the details of the underlying network topology have an impact on the availability of network services. Especially, when moving from small to larger networks, beyond increasing the length of end-to-end path, there is evidence that shared risk link groups (SRLGs) will more probably be present and negatively impact availability. (A shared risk link group is a structure containing two or more logically disjoint links that share a physical location and are subject to failing at the same time.) In particular, Segovia, Calle and Villa analyzed the network availability for six different physical network topologies [10], differing in number of nodes and links, average node degree, network diameter, link length and other indices. They inferred that large topologies have very different average availability values from smaller topologies, and that difference in availability in smaller topologies could not be observed.

Meanwhile, there has been considerable research on the impact of SRLGs on network availability. Doucette et al. studied capacity requirements in the network in presence of SRLGs, and proposed a design model that included elimination of known SRLGs within budget limits and covering others with additional capacity [11]. We previously analyzed the impact of SRLG length variation on network availability using a specific test topology, and concluded that unavailability increases linearly with increasing SRLG length [12].

Building upon the work described above, in this paper we compare six physical topology models in terms of resulting network and connection availability. We specifically evaluate availability in presence of SRLGs against the scenario where no SRLGs are present. While failure dependency – inherent in SRLGs – makes analytical computation of availability complicated, we make use of Monte Carlo simulation utilizing optical network availability model [12] implemented by network simulator ns-3 [13], [14] to obtain results. We expect that there will be a significant difference in network availability for different topology models, and that the impact of SRLGs on different topologies will also considerably vary. We furthermore anticipate being able to correlate impact of SRLGs with certain topological properties.

The paper is organized as follows: in Section II we describe the topology models we have chosen for this study, in Section III we refer to the topology implementation details and statistical properties and in Section IV we briefly cover basics of availability analysis in the field of optical networks. Finally, in Section V we present the case study and the simulation results, while in Section VI we conclude with some directions and plans for future work.

## II. NETWORK TOPOLOGIES

The recent appearance of geographic graph generators allows the creation of several realistic synthetic graphs for extensive simulation studies. Such graph models generate topologies that fairly fit the observed real-world non-trivial topological features that are neither purely regular nor purely random. The most well-established physical level models are the Random Geometric Graph model [15], the Gabriel Graph model [16], the Relative Neighborhood Graph model [17], the K-Nearest Neighbor Graph model [18], the Waxman model [19] and the Spatial Barabási-Albert (or Preferential Attachment) model [20]–[22], additionally to many others, less popular, such as the Geographical Threshold Graph model [23], [24], the Transit-Stub [25], the KU-LoCGen [26], the HINT [27], and so on [28]. However, the above topology generators do not take into account network design objectives and constraints such as minimizing the latency, dimensioning the links, adding redundancy or minimizing the network budget. Instead, their main objective is to be realistic in terms of fitting the properties of observed real networks, so they serve different purpose than algorithms for optimized physical topology generation, e.g. [29].

Apart from the inherent graph-theoretic interest when studying spatial graph generation, the evaluation of such topologies

under failure scenarios always can provide critical information about the network behavior and moreover contributes to understanding the network availability. Regarding the SRLG related literature, the usage of synthetic graph topologies is somehow narrow and rather limited to the Waxman and Barabási-Albert models. Particularly, in [30] the authors presented an IP fast reroute mechanism for SRLG failures in routing protocols without global topology information. Through simulations on both Waxman and Barabási-Albert topologies, they confirmed that their mechanism can achieve a repair coverage close to 100% for different SRLG size. Furthermore, for the experiment setup in [31], in which a tool for network fault diagnosis was presented, the authors used either Waxman or Barabási-Albert as a physical connectivity pattern. As well, the authors in [3] used synthetic network topologies based on the Waxman model, together with some publicly available real topologies, for their evaluation methods of IP fast reroute schemes. Likewise, in [4] where the fault localization problem was considered, the authors employed Waxman-based topologies along with real-world topologies in their extensive simulations with the intention of demonstrating the effectiveness of the proposed monitoring technique. Besides, in [5] the performance of the proposed fast reroute scheme was validated under a variety of real and synthetic Waxman topologies. Similarly, real and Waxman graphs, jointly with 2-level hierarchical graphs and purely random graphs were used in [6] for experiments on efficient load balancing under a wide range of failure scenarios.

### A. Random Geometric Graph model

A random geometric graph is a random undirected graph drawn on a bounded region, e.g. the unit square or on any  $d$ -dimensional Euclidean space. It is generated as follows [15]. First  $n$  nodes are placed (independent and identically distributed) uniformly at random on the region. Consequently for some specific distance threshold parameter  $r$ , nodes  $i$  and  $j$  are connected if and only if the distance between them is at most  $r$ :

$$d(i, j) \leq r \quad (1)$$

where  $d(i, j)$  is the Euclidean distance between the two nodes  $i$  and  $j$ . Modeling random networks in this way is simple and easy to implement, and sometimes a more realistic alternative to the classical random graph models of Erdős and Rényi [32].

### B. Gabriel Graph model

The Gabriel graphs are named after K.R. Gabriel, who introduced them in a paper with R.R. Sokal in 1969 [16]. In this connection scheme, two nodes are connected directly if and only if there are no other nodes that fall inside the circle (or sphere in three dimensions) associated with the diameter that has the two nodes as endpoints. Mathematically, two nodes  $i$  and  $j$ , from a set of  $n$  nodes, are connected if the square of the distance between them is less than the sum of the squared distance between each of these points and any other point  $k$ . That is an undirected graph is constructed by

adding edges between nodes  $i$  and  $j$  if for all nodes  $k$ ,  $k \neq i, j$ , where  $d$  expresses the Euclidean distance:

$$d(i, j)^2 \leq d(i, k)^2 + d(j, k)^2 \quad (2)$$

The Gabriel graphs are useful in modeling graphs with geographic connectivity that resemble grids [16]. These synthetic graphs when compared to AT&T, Level 3, Sprint, and other physical networks, were found to most closely capture the grid-like structure and at the same time achieve the smallest cost among all of the graph models considered in [9]. Moreover, in [33] Bell Atlantic confirmed the Gabriel graph model of their wire centers in Pennsylvania to be remarkably similar to the topology of their inter-office network.

### C. Relative Neighborhood Graph model

In computational geometry, the relative neighborhood graph is a subgraph of the Gabriel graph. It is an undirected graph created by connecting two nodes  $i$  and  $j$ , from a set of  $n$  nodes, by an edge whenever there does not exist a third node  $k$  that is closer to both  $i$  and  $j$  than they are to each other [17]. In other words an edge is formed between  $i$  and  $j$  if and only if there is no other node in the interior of the intersection (lune) of the two circles, one with center at  $i$  and the other centered at  $j$ , with the same radius  $d(i, j)$ . Formally, the relative neighborhood graph of a set of nodes in the plane is defined as follows: Two nodes  $i$  and  $j$  define an edge when for all nodes  $k$ ,  $k \neq i, j$ , where  $d$  expresses the Euclidean distance:

$$d(i, j) \leq \max\{d(i, k), d(j, k)\} \quad (3)$$

### D. $K$ -Nearest Neighbor Graph model

The  $k$ -nearest neighbor graph is a graph in which two nodes  $i$  and  $j$ , from a set of  $n$  nodes, are connected by an edge, if the distance between  $i$  and  $j$  is among the  $k$ -th smallest distances from  $i$  to all other nodes [18]. The resulting set of edges represents the outcome of the  $k$  nearest neighbors query for each node. The directions of the edges may be ignored to lead to an undirected graph.

### E. Waxman Graph model

The Waxman topology model incorporates location information into random graphs and was introduced by Waxman [19] as a geographic model for the growth of a computer network. In this model the  $n$  nodes of the network are uniformly distributed in the plane and they are connected based on a probability derived from the geographical distance between the nodes, in contrast to the Erdős–Rényi model where the probability is fixed [32]. The probability to have an edge between nodes  $i$  and  $j$  is given by:

$$P(i, j) = \alpha e^{-\frac{d(i, j)}{\beta L}} \quad (4)$$

where  $\alpha, \beta \in (0, 1]$ ,  $d(i, j)$  is the Euclidean distance from  $i$  to  $j$ , and  $L$  denotes the maximum distance between any two nodes. An increase in the parameter  $\alpha$  increases the edge density, while an increase in  $\beta$  yields a larger ratio of long edges to short edges. The output of this model is an undirected graph with a higher probability for edges between two nodes that are close compared to two nodes further apart.

### F. Spatial Barabási-Albert Graph model

The Barabási-Albert model generates scale-free networks using a preferential attachment mechanism [34]. It implements the key concept that highly connected vertices are likely to become even more connected. Each new node in this evolving model is connected to a number of existing nodes with a probability proportional to the number of links that the existing nodes already have.

Starting from the Barabási-Albert model, authors in [20] developed a spatial version of the model. In this spatial model, the network grows until  $n$  nodes have been created. For a fixed integer  $m \geq 1$ , each new node is given  $m$  links on arrival. These new connections are not chosen uniformly; the new node attaches itself to an existing node with a probability that is proportional to the latter's connectivity, as suggested by Barabási and Albert [34]. Furthermore, since the cost of connecting two nodes increases with geographical distance, the probability that the new node connects to the already connected node is inversely dependent on their distance. Hence, well-connected nodes tend to become even better connected with a bias towards less distant nodes as the network evolves. The probability that the new node  $i$  connects to node  $j$  is:

$$P(i, j) = \frac{k_j}{\sum_j k_j} \frac{1}{(d(i, j))^\alpha} \quad (5)$$

where  $k$  is the degree of the node,  $d$  is the Euclidean distance and  $\alpha \geq 0$  is a parameter for controlling the distance effects. The probabilities are to be normalized such that the sum of all probabilities adds up to one.

This model leads to undirected graphs that take into account the effect of geographical distance and in the same time are characterized by the presence of few nodes with a large number of links (called hubs), while most nodes only have few ones.

## III. IMPLEMENTATION AND STATISTICAL PROPERTIES OF THE CHOSEN MODELS

In this study, we choose a  $1000 \times 1000$  (i.e. kilometers) square plane as the 2-dimensional Euclidean space where we place  $n = 100$  nodes (independent and identically distributed) uniformly at random. Two out of the six models are parameterless (the Gabriel and the Relative Neighborhood models) using only node locations as input, while the rest require at least one parameter. We choose these parameters upholding biconnectivity as a prerequisite. A biconnected graph is a connected graph (no isolated nodes) that if any node or edge were to be removed, the graph will remain connected<sup>1</sup>. This property is valuable in maintaining a graph with a two-fold redundancy, to avoid disconnection upon the deletion of a single node/edge. On the grounds of this redundancy property, the use of biconnected graphs is very essential in the field of networking and especially SRLG related studies. Simultaneously, we select the parameters' values to minimize the

<sup>1</sup>When measuring the biconnectivity on the Relative Neighborhood graphs, leaf nodes are not considered as articulation points since when a leaf is deleted from a graph, the rest of the graph remains connected.

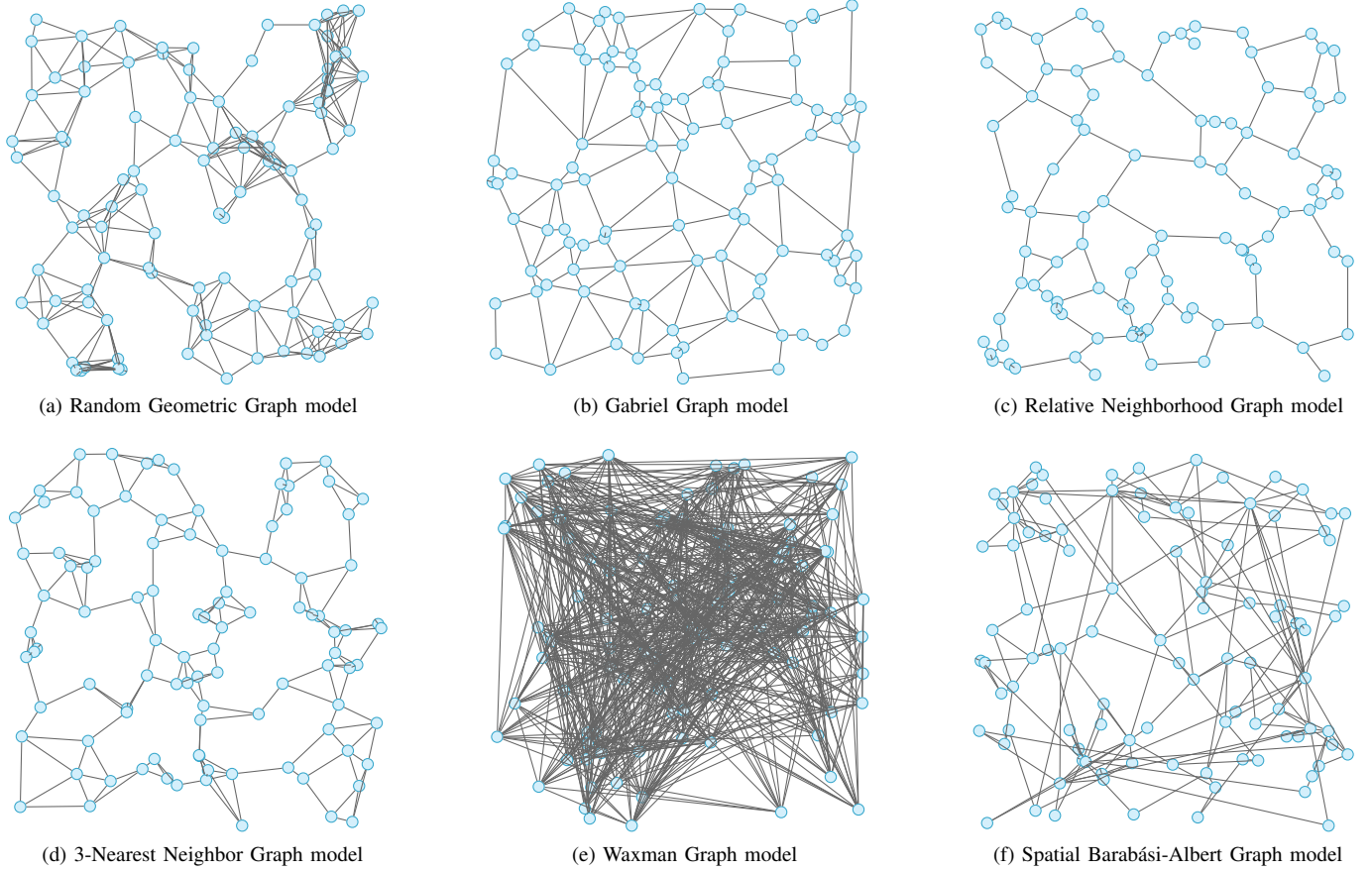


Figure 1. Visualizations of instances of the six topology types.

total wiring of the graph, which is another realistic assumption for constructing networks in the physical level. In particular, for the Random Geometric model  $r = 150$ , for the  $k$ -Nearest Neighbor model  $k = 3$ , for the Waxman model  $\alpha = 0.6$  and  $\beta = 0.3$ , for the Spatial Barabási-Albert model  $m = 2$  and as derived by the empirical analysis in [20] the value for  $\alpha = 3$ . We generate and test families of 100 networks of each of the above models. In Figure 1 typical topologies of each model are observed.

The basic statistical properties of such topologies are referred here: the average shortest path, the diameter, the average clustering coefficient, the degree (mean, minimum, maximum). The average shortest path or average geodesic path length is defined as the average number of steps along the shortest paths for all possible pairs of network nodes. The diameter of a network is the length (in number of edges) of the longest shortest path between any two nodes in the network. The average clustering coefficient is defined as the average of all  $n$  local clustering coefficients  $C_i$ , where  $C_i = \frac{\text{number of triangles connected to node } i}{\text{number of triples centered on node } i}$ . In particular, a triangle indicates that two neighbors of a node are also connected by an edge, while the number of triples indicates the number of permitted edges between the neighbors of a node. The degree of a node is the number of edges directly connected to the

node. The total wiring is defined as the sum of edge lengths, while the average link length is defined as the ratio of the summation of all edge lengths to the number of edges, both measured in kilometers here.

In Table I, the basic statistical properties for the six topologies under study are presented. All values are rounded to the nearest tenth decimal, while the standard deviation appears in the parentheses. What turns out notably significant is that the Relative Neighborhood graphs, along with the 3-Nearest Neighbor and the Gabriel graphs show a considerably lower cost in terms of total wiring. The Gabriel graphs have already been found to closely capture the grid-like structure of physical-level networks and at the same time achieve a feasible cost [9]. These three models which have an advantage in total wiring are also the best in terms of average link length, but the worst in the average shortest path and diameter properties. Even though, the main difference among these three models is that the 3-Nearest Neighbor demonstrates a quite higher average clustering coefficient. Although the rest three models are more common in the literature as synthetic topology generators, they produce graphs with high or extremely high total wiring, i.e. Waxman, and a variety of property values. The Waxman graphs appear to have a very low average shortest path and diameter due to their high

Table I  
 BASIC STATISTICAL PROPERTIES FOR THE SIX TOPOLOGIES STUDIED (NODES=100, PLANE=1000 × 1000). STANDARD DEVIATION APPEARS IN THE PARENTHESES.

Topology model	Number of edges	Average shortest path (hops)	Diameter	Average clustering coefficient	Total wiring (km)	Average link length (km)	Mean node degree	Min node degree	Max node degree
Random Geometric Graph	306.1 (20.9)	5.8 (0.4)	10.6 (1.6)	0.6 (0)	30577.2 (2149.8)	99.9 (1.6)	6.1 (0.4)	2.0 (0)	11.7 (1.5)
Gabriel Graph	180.5 (6.3)	6.0 (0.2)	11.1 (1.7)	0.2 (0)	17813.2 (930.2)	98.7 (2.9)	3.6 (0.1)	2.0 (0.2)	6.5 (0.6)
Relative Neighborhood Graph	120.4 (3.1)	8.5 (0.5)	16.2 (2.1)	0 (0)	9757.5 (532.9)	81.0 (2.8)	2.4 (0.1)	1.0 (0)	3.9 (0.2)
3-Nearest Neighbor Graph	189.8 (4.0)	7.8 (0.6)	14.0 (2.2)	0.5 (0)	16530.9 (679.6)	87.1 (2.8)	3.9 (0.1)	3.0 (0)	6.6 (0.7)
Waxman Graph	943.2 (42.4)	1.9 (0)	2.8 (0.4)	0.2 (0)	355024.3 (19025.9)	376.4 (12.1)	18.9 (0.9)	7.7 (1.4)	31.9 (2.8)
Spatial Barabási-Albert Graph	197.0 (0)	3.4 (0.1)	5.7 (0.6)	0.3 (0.1)	36247.2 (2031.7)	184.0 (10.3)	3.9 (0)	2.0 (0.2)	18.1 (3.3)

number of edges, while the Random Geometric graphs show the highest average clustering coefficient. Last, the Spatial Barabási-Albert graphs result in low average shortest path and diameter while maintaining a relatively low mean node degree, compared to the aforementioned two models.

Unfortunately, the diversity in the values of statistical properties (i.e. number of edges, total wiring) may raise potential concerns about performing a legitimate comparison. However, this is both reasonable and unavoidable since each model has – by definition – specific limitations and not all its attributes can be controlled concurrently. For instance, we cannot impose the generation of fewer edges on the Waxman model without letting the existence of isolated nodes. Respectively, in the Random Geometric model we cannot produce a biconnected graph with a lesser value in  $r$ , than the one already assigned. This is more evident in the parameterless models, where – by default – we are unable to control the output traits. In short, holding the same number of nodes, retaining biconnectivity and then minimizing cost (where applicable), are the requirements for inclusion in the comparison, albeit we still observe extremely diverse values in some models (e.g. Waxman), which are kept in our analysis due to their prevalence in the related literature.

#### IV. OPTICAL NETWORK AVAILABILITY ANALYSIS

Network availability is a probability that a repairable system will be in operating state at a random moment in time. It can be computed by both analytical and simulation methods. The analytical method uses component mean time to failure (MTTF) and mean time to repair (MTTR) to compute the network availability, by considering the availability of logical connections established in the network. Availability of logical connections can be computed by computing availability of paths they use, which can furthermore be reduced to considering availability of network components in the path. Analytical method relies on serial and parallel relationships between components of a path or paths used by a connection, but the relationship among components can become complex in

presence of failure dependencies, which are neither serial nor parallel relationships.

Unavailability is defined as a complement of availability. Since availability values are usually very close to 1 (or 100%), it is much easier to compare availability results based on the order of magnitude in unavailability difference.

Monte Carlo simulation can be used for the estimation of network availability. Particularly, it uses random numbers to generate times to failure and times to repair for components in the network, based on their MTTF and MTTR values. Failure and repair events are then handled by the component model implemented in a network simulator. It is possible to make a failure (or a repair) in a particular component to affect other components in a certain way. More specifically, this makes it possible to model complex neither serial nor parallel relationships such as failure dependency.

The network model we use is implemented by discrete event network simulator ns-3. More details of the model and its implementation can be found in [12].

#### V. CASE STUDY

For the evaluation of network availability we use 100 instances for each of the six physical topology models described above, totaling to 600 different physical topologies.

##### A. Scenario description

We evaluate scenarios where all pairs of nodes have bidirectional logical connections, each having working and spare path. As each test network has 100 nodes, 4950 bidirectional connections are established. A more detailed traffic model based on either population or other geographical properties could as well be used instead of the full mesh connection scheme. Since we use synthetic topologies, such a model would require another randomly generated parameter - or set of parameters - to be introduced. This in turn would affect the results, and therefore make the correlations between topological properties and availability less evident. Additionally, although the effect of node failures could be explored as well,

it is considered beyond the scope of this paper and therefore the network nodes are assumed to be fully reliable.

We take cables having failure rate of 310 FIT per kilometer (1 FIT = 1 failure in  $10^9$  hours), which includes fiber and inline amplifier failures [35]. We assume MTTR to be 12 hours and nodes in the network to be ideal<sup>2</sup> (have availability equal 1). We further consider that once a failure of a cable occurs, then all contained fibers will also fail.

Logical connection is considered to be up if at least one of the paths it uses is so, while otherwise it is considered down. A path is regarded to be up if all the contained links are in working state, or in other words, none of the contained links in the path is in a failed state.

We use two measures of network availability as follows:

- $s,t$ -availability, the smallest of all logical connection availabilities,
- $g$ -availability, the probability that all logical connections in the network are up at a random time.

We now also define  $s,t$ -unavailability and  $g$ -unavailability as complements of  $s,t$ -availability and  $g$ -availability (respectively).

The SRLG model which has been used is the one described in [12]. In particular, this model assumes that each SRLG contains parts of two or more cables sharing a physical location. If the cable part contained in SRLG fails, there is a specific probability that the other cables are damaged too. Notably, this probability is set to be 0.7 [36]. It is additionally assumed that all cables are repaired in the common part upon repair.

We simulate the scenarios with no SRLGs and 200 SRLGs present in the network. In the case where SRLGs are present in the network, their length is normally distributed with mean 3.0 km, and each SRLG contains two cables. We take all SRLGs to be coincident, meaning that cables contained in SRLG share a common node. We use SRLG-aware routing that sets up working and spare paths for each logical connection which are both link and SRLG-disjoint if possible, and only link-disjoint otherwise.

For each topology instance we conduct 20 runs of Monte Carlo simulation lasting  $10^9$  hours of simulated time, resulting in 2000 simulation iterations done per physical topology model for each scenario.

### B. Simulation results and discussion

Simulation results presented in Figures 2 and 3 are obtained by computing mean value and standard deviation on 2000 runs for each topology model and each scenario, as well. It is obvious that there is a significant difference both in  $g$ - and  $s,t$ -unavailabilities among these models.

To begin with, the Relative Neighborhood model has the highest unavailability among the models presented here. This fact can be fairly perceptible given the presence of leaves in

<sup>2</sup>Our model allows configuration of MTTF and MTTR for optical network components contained in nodes. Failures of network components could be considered as well as link failures. However, such consideration falls outside the scope of this paper.

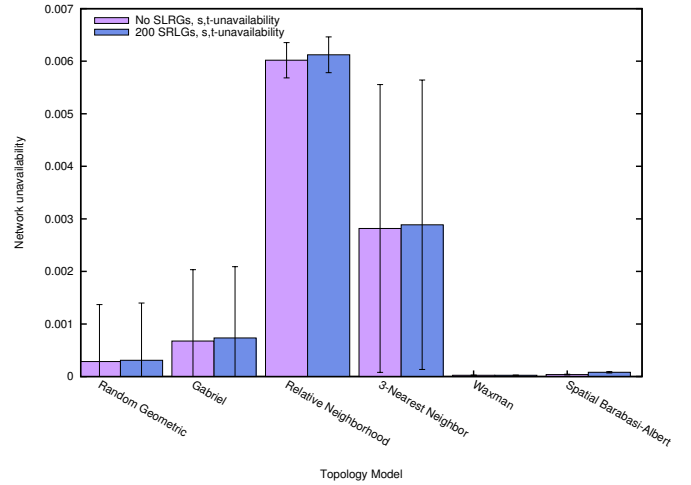


Figure 2. Simulation results  $s,t$ -unavailability: comparison of scenarios with no SRLGs to scenarios with SRLGs present in the network.

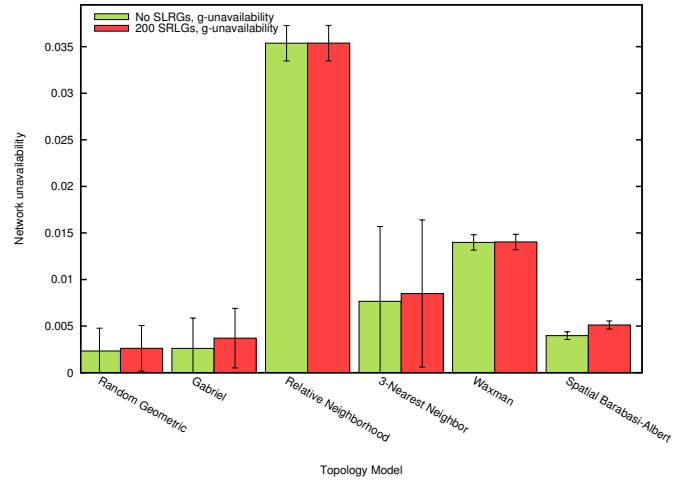


Figure 3. Simulation results  $g$ -unavailability: comparison of scenarios with no SRLGs to scenarios with SRLGs present in the network.

the graph, and also by the zero value in the average clustering coefficient. In addition, this model produces graphs with lower number of edges than other models, which results in inability to find link-disjoint spare paths for some connections. This inability could also explain negligible difference in  $g$ -unavailability in presence of SRLGs; if it is not possible to find a backup path for some logical connection that is link-disjoint, it will certainly not be possible to find one that is both link- and SRLG-disjoint. On the other hand, the increase in  $s,t$ -unavailability can be explained by the increase in average backup path length in presence of SRLGs for those logical connections whose SRLG-disjoint paths could be found.

Continuing, the Random Geometric model has the lowest  $g$ -unavailability and is among the lowest with regard to  $s,t$ -unavailability. Larger number of edges generally induce a larger number of possible backup paths. In parallel, a larger number of possible backup paths results in links being shared

by fewer number of backup paths set up when establishing logical connections. This in turn results in a single failure on average affecting lower number of logical connections, which results in low value for  $s,t$ -unavailability. Relatively high standard deviation can be explained by randomness inherent in the model.

The Gabriel model is similar to the Random Geometric in terms of  $g$ -unavailability, but at a much lower number of edges and total wiring. This is reflected in the increase of  $s,t$ -unavailability, since the number of possible backup paths in the Gabriel model is lower compared to the Random Geometric model. We can additionally observe that lower number of edges compared to that of the Random Geometric model leads to a more negative SRLGs impact on  $g$ -unavailability, due to the fact that SRLG-disjoint backup paths are more unlikely to exist on average.

For the Waxman model, the relatively low  $s,t$ -unavailability can be explained by many possible paths due to having almost an order of magnitude more edges than other models. Once again, we deem it necessary to emphasize that despite this last finding, still, the Waxman model is frequently common in literature and thus it is included here for comparison aims. Besides, the relatively high  $g$ -unavailability could be attributed to large total wiring and therefore more failure occurrences in time, affecting some of the logical connections. Furthermore, we can observe that in the Waxman model SRLGs have a negligible effect on unavailability; due to many possible paths between two nodes, it is very likely that SRLG-disjoint paths can be found. Negative effect of SRLG failure resulting in two concurrent logical link failures is still present, however.

The 3-Nearest Neighbor model shows much lower  $s,t$ -unavailability to Relative Neighborhood, albeit on the same order of magnitude, which is plausibly expected due to the larger number of edges. There is also an even greater improvement in terms of  $g$ -unavailability, which however results in noticeable impact of SRLGs. As also with Random Geometric model, high standard deviation can be explained by randomness that is inherent in the model.

Moreover, the Spatial Barabási-Albert model indicates very good performance in terms of both  $s,t$ - and  $g$ -unavailability, as well. Similarly to the Waxman model, the relatively high total wiring results in a very low  $s,t$ -unavailability but this does not hold also for  $g$ -unavailability. Additionally, the observation about the effect of SRLGs on the Gabriel model does also hold for the Spatial Barabási-Albert.

Besides, and since the Gabriel model has been found to most closely fit real physical networks [9], the usage of different topology models in availability related experiments could lead to availability miscalculation. Thus, the utilization of models such as the Waxman, the Spatial Barabasi-Albert or the Random Geometric would underestimate the  $s,t$ -unavailability, while the usage of models such as the Relative Neighborhood or the 3-Nearest Neighbor would contrary result in an overestimation of this metric. Regarding the estimation of  $g$ -unavailability, the usage of the Random Geometric model would probably underrate it, while the usage of any other

model, among the considered ones, would on the other hand exaggerate its value.

## VI. CONCLUSIONS

In this paper we implemented and used six different physical topology models for investigating their influence on optical telecommunication network availability. We anticipated observing an apparent difference in availability of logical connections and a significant difference in the impact of SRLGs on network availability for the considered topology models. Eventually, the results actually did fulfill the above expectations. On top of that, the findings elaborated above also indicate a coupling between particular topological metrics and optical network availability, albeit not a trivial one. Average shortest path and diameter appear to have a critical effect on  $s,t$ -availability, while regarding  $g$ -availability it turns up to be influenced by the average shortest path and diameter in combination with the total wiring as well. Nonetheless, any possible correlation between those metrics and network availability seems to be non-trivial and no definitive conclusion has so far been reached about it.

In terms of future work, it would be quite intriguing to further examine and explain the correlations between a richer set of topological metrics and availability measurements. Since it is unlikely that such correlations are trivial ones, let alone including the presence of SRLGs, we are convinced that this research direction will eventually contribute to a better understanding of the network availability determinants. Finally, the challenging study of effective (in terms of network availability) network topology construction based on such results is a direction which warrants further attention and research.

## REFERENCES

- [1] S. De Maesschalck, D. Colle, I. Lievens, M. Pickavet, P. Demeester, C. Mauz, M. Jaeger, R. Inkrät, B. Mikac, and J. Derkacz, "Pan-european optical transport networks: an availability-based comparison," *Photonic Network Communications*, vol. 5, no. 3, pp. 203–225, 2003.
- [2] A. Betker, C. Gerlach, R. Hülsermann, M. Jäger, M. Barry, S. Bodamer, J. Späth, C. Gauger, and M. Köhn, "Reference transport network scenarios," *MultiTeraNet Report*, July, 2003.
- [3] T. Cicic, A. F. Hansen, A. Kvalbein, M. Hartmann, R. Martin, M. Menth, S. Gjessing, and O. Lysne, "Relaxed multiple routing configurations: Ip fast reroute for single and correlated failures," *Network and Service Management, IEEE Transactions on*, vol. 6, no. 1, pp. 1–14, 2009.
- [4] S. Ahuja, S. Ramasubramanian, and M. Krunz, "Srlg failure localization in optical networks," *IEEE/ACM Transactions on Networking (TON)*, vol. 19, no. 4, pp. 989–999, 2011.
- [5] K. Xi, H. J. Chao, and C. Guo, "Recovery from shared risk link group failures using ip fast reroute," in *Computer Communications and Networks (ICCCN), 2010 Proceedings of 19th International Conference on*. IEEE, 2010, pp. 1–7.
- [6] M. Suchara, D. Xu, R. Doverspike, D. Johnson, and J. Rexford, "Network architecture for joint failure recovery and traffic engineering," in *Proceedings of the ACM SIGMETRICS joint international conference on Measurement and modeling of computer systems*. ACM, 2011, pp. 97–108.
- [7] D. Maniadakis, A. Balmpakakis, and D. Varoutas, "On the temporal evolution of backbone topological robustness," in *Network and Optical Communications (NOC), 2013 18th European Conference on and Optical Cabling and Infrastructure (OC&I), 2013 8th Conference on*. IEEE, 2013, pp. 129–136.

- [8] L. A. Schintler, S. P. Gorman, A. Reggiani, R. Patuelli, A. Gillespie, P. Nijkamp, and J. Rutherford, "Complex network phenomena in telecommunication systems," *Networks and Spatial Economics*, vol. 5, no. 4, pp. 351–370, 2005.
- [9] E. K. Çetinkaya, M. J. Alenazi, Y. Cheng, A. M. Peck, and J. P. G. Sterbenz, "On the Fitness of Geographic Graph Generators for Modelling Physical Level Topologies," in *Proceedings of the 5th IEEE/IFIP International Workshop on Reliable Networks Design and Modeling (RNDM)*, Almaty, September 2013.
- [10] J. Segovia, E. Calle, and P. Vila, "Availability analysis of gmpls connections based on physical network topology," in *Optical Network Design and Modeling, 2008. ONDM 2008. International Conference on*. IEEE, 2008, pp. 1–6.
- [11] J. Doucette, W. D. Grover *et al.*, "Capacity design studies of span-restorable mesh transport networks with shared-risk link group (srlg) effects," *SPIE Opticomm. Citeseer*, 2002.
- [12] V. Miletic, B. Mikac, and M. Dzanko, "Impact evaluation of physical length of shared risk link groups on optical network availability using monte carlo simulation," in *Network and Optical Communications (NOC), 2013 18th European Conference on and Optical Cabling and Infrastructure (OC&I), 2013 8th Conference on*. IEEE, 2013, pp. 249–255.
- [13] T. R. Henderson, M. Lacage, G. F. Riley, C. Dowell, and J. Kopena, "Network simulations with the ns-3 simulator," *SIGCOMM demonstration*, 2008.
- [14] T. R. Henderson, S. Roy, S. Floyd, and G. F. Riley, "ns-3 project goals," in *Proceeding from the 2006 workshop on ns-2: the IP network simulator*. ACM, 2006, p. 13.
- [15] M. Penrose, *Random geometric graphs*. Oxford University Press Oxford, 2003, vol. 5.
- [16] K. R. Gabriel and R. R. Sokal, "A new statistical approach to geographic variation analysis," *Systematic Biology*, vol. 18, no. 3, pp. 259–278, 1969.
- [17] G. T. Toussaint, "The relative neighbourhood graph of a finite planar set," *Pattern recognition*, vol. 12, no. 4, pp. 261–268, 1980.
- [18] D. Eppstein, M. S. Paterson, and F. F. Yao, "On nearest-neighbor graphs," *Discrete & Computational Geometry*, vol. 17, no. 3, pp. 263–282, 1997.
- [19] B. M. Waxman, "Routing of multipoint connections," *Selected Areas in Communications, IEEE Journal on*, vol. 6, no. 9, pp. 1617–1622, 1988.
- [20] S. Vinciguerra, K. Frenken, and M. Valente, "The geography of internet infrastructure: an evolutionary simulation approach based on preferential attachment," *Urban Studies*, vol. 47, no. 9, pp. 1969–1984, 2010.
- [21] A. D. Flaxman, A. M. Frieze, and J. Vera, "A geometric preferential attachment model of networks," *Internet Mathematics*, vol. 3, no. 2, pp. 187–205, 2006.
- [22] S.-H. Yook, H. Jeong, and A.-L. Barabási, "Modeling the internet's large-scale topology," *Proceedings of the National Academy of Sciences*, vol. 99, no. 21, pp. 13 382–13 386, 2002.
- [23] N. Masuda, H. Miwa, and N. Konno, "Geographical threshold graphs with small-world and scale-free properties," *Physical Review E*, vol. 71, no. 3, p. 036108, 2005.
- [24] M. Bradonjic, A. Hagberg, and A. G. Percus, "The structure of geographical threshold graphs," *Internet Mathematics*, vol. 5, no. 1–2, pp. 113–139, 2008.
- [25] K. L. Calvert, M. B. Doar, and E. W. Zegura, "Modeling internet topology," *Communications Magazine, IEEE*, vol. 35, no. 6, pp. 160–163, 1997.
- [26] A. Jabbar, Q. Shi, E. Cetinkaya, and J. P. Sterbenz, "Ku-locgen: Location and cost-constrained network topology generator," ITTC Technical Report ITTC-FY2009-TR-45030-01, The University of Kansas, Lawrence, KS, Tech. Rep., 2008.
- [27] X. Ma, S. Kim, and K. Harfoush, "Towards realistic physical topology models for internet backbone networks," in *High-Capacity Optical Networks and Enabling Technologies (HONET), 2009 6th International Symposium on*. IEEE, 2009, pp. 36–42.
- [28] C. Pavan, R. M. Morais, J. R. Ferreira da Rocha, and A. N. Pinto, "Generating realistic optical transport network topologies," *Journal of Optical Communications and Networking*, vol. 2, no. 1, pp. 80–90, 2010.
- [29] H. Liu and F. A. Tobagi, "Physical topology design for all-optical networks," *Optical Switching and Networking*, vol. 5, no. 4, pp. 219–231, 2008.
- [30] Y. Li and M. G. Gouda, "Ip fast reroute in networks with shared risk links," in *NETWORKING 2010*. Springer, 2010, pp. 213–226.
- [31] S. Kandula, D. Katabi, and J.-P. Vasseur, "Shrink: A tool for failure diagnosis in ip networks," in *Proceedings of the 2005 ACM SIGCOMM workshop on Mining network data*. ACM, 2005, pp. 173–178.
- [32] P. Erdős and A. Rényi, "On the evolution of random graphs," *Publ. Math. Inst. Hungar. Acad. Sci.*, vol. 5, pp. 17–61, 1960.
- [33] G. Cai, S. Hirtle, and J. Williams, "Mapping the geography of cyberspace using telecommunications infrastructure information," *TeleGeo*, pp. 6–7, 1999.
- [34] A.-L. Barabási and R. Albert, "Emergence of scaling in random networks," *science*, vol. 286, no. 5439, pp. 509–512, 1999.
- [35] D. A. Mello, D. A. Schupke, M. Scheffel, and H. Waldman, "Availability maps for connections in wdm optical networks," in *Design of Reliable Communication Networks, 2005.(DRCN 2005). Proceedings. 5th International Workshop on*. IEEE, 2005, pp. 8–pp.
- [36] L. Wosinska, D. Colle, P. Demeester, K. Katrinis, M. Lackovic, O. Lapevic, I. Lievens, G. Markidis, B. Mikac, M. Pickavet, B. Puype, N. Skorin-Kapov, D. Staessens, and A. Tzanakaki, "Network resilience in future optical networks," *Towards Digital Optical Networks*, pp. 253–284, 2009.